

SPATIAL ESTIMATION OF BIOCHEMICAL PARAMETERS OF LEAVES WITH HYPERSPECTRAL IMAGER

Takahiro ENDO*, Yoshifumi YASUOKA* and Masayuki TAMURA**

*Yasuoka Lab., Institute of Industrial Science (IIS), the University of Tokyo

4-6-1 Komaba, Meguro-ku, Tokyo 153-8505, Japan

Tel: +81-3-5452-6415 Fax: +81-3-5452-6410

E-mail: tendo@iis.u-tokyo.ac.jp

**National Institute for Environmental Studies,

16-2, Onogawa Tsukuba Ibaraki 305-0053, Japan

KEYWORDS: Hyperspectral imager, Biochemical parameter, Chlorophyll *a*, Red edge position, RWC

ABSTRACT: This paper investigates a spatial measurement method of chlorophyll *a* concentration of leaves from spectral characteristics using a hyperspectral imager with AOTF (Acousto-Optic Tunable Filter) in 400 – 1000 nm wavelength range, with a 5 nm wavelength intervals, respectively. A distribution of chlorophyll *a* concentration in the entire leaf area was estimated based on experiments. *Ginkgo biloba* and *Zelkova serrata* were collected from a field in IIS, the University of Tokyo. Chlorophyll *a* concentration was determined by quantitative analysis at our laboratory. In addition, spectral characteristics were measured at the laboratory darkroom. The standard deviation of spectral reflectance of the leaf in the neighborhood of red edge position was very small. The determination of coefficient between chlorophyll *a* concentration ($\mu\text{g}/\text{cm}^2$) and the first derivative spectral reflectance of each leaf measured in the neighborhood of red edge position was $r^2=0.85$ and $r^2=0.79$, respectively. The RMS error of the estimated chlorophyll *a* concentration in the two leaves was $4.80 \mu\text{g}/\text{cm}^2$ and $3.05 \mu\text{g}/\text{cm}^2$, respectively. On the other hand, relationship between relative water content (RWC) of leaf and spectral characteristics was also investigated using the hyperspectral imager and the hyperspectral meter. However, it was found that there wasn't any recognizable pattern across the two leaves.

1. INTRODUCTION

It is quite important to estimate spatial distribution of biochemical parameters in terrestrial ecosystem such as chlorophyll, nitrogen, LAI, photosynthetic rate and NPP. For instance, the spatial distribution of measurement of terrestrial parameters is needed to estimate carbon flux of crop area, forest area and so on. In recent year, the field of remote sensing has made a progress in developing methods that relate remotely sensed data to regional estimates of a number of essential ecosystem parameters. Chlorophyll concerning with plant activity has been investigated for a number of years, and been reported by various researchers. For example, strong correlations exist between remotely sensed data and the concentration of many biochemical substances within vegetation canopies (Paul et al., 1997). The chlorophyll concentration of leaf is negatively proportional at 680 nm wavelength and positively proportional to the point of maximum slope between 690 – 740 nm of spectral reflectance (Miller et al., 1997). This point is known as the “red edge” of plant reflectance. Besides, estimation of biochemical properties of canopy has been reported especially using airborne data within short-wave infrared wavelengths. Lee F. Johnson et al. found correspondence between the first derivative spectral reflectance from the Airborne Visible/Infrared Imaging Spectrometer (AVIRIS) and concentrations of both chlorophyll and total nitrogen ($r^2=0.71$ and $r^2=0.85$, respectively) along a vegetation transect in Oregon. The first derivative reflectance of AVIRIS data predicted chlorophyll, nitrogen, lignin, and cellulose concentrations ($r^2=0.96$ $r^2=0.94$ $r^2=0.93$, and $r^2=0.61$, respectively) at a slash pine plantation, Florida (Rosemary et al., 1999). However, as the resolution of airborne data is several square meters, it is difficult to evaluate the effect of shadow, overlapping of leaves, stem and position of leaves from the measured hyperspectral image. On the other hand, estimation of photosynthetic rate could be estimated from chlorophyll *a* or nitrogen concentration using the data of hyperspectral meter in ground experiment (Endo et al., 2000).

Hence, it is necessary to link the pixel resolution to the ground measurements, with this in mind, we used a portable hyperspectral imager, which is a useful tool to evaluate the effect of shadow, stem and overlap of leaves. The aim of this study was to investigate the appropriateness in estimating the biochemical parameters, such as chlorophyll *a* and to examine the effect of shadow on spectral characteristics.

2. MATERIALS AND METHODS

2.1 Species, Sample Collection

Two species were collected for this study from the grounds of IIS, the University of Tokyo. One was *Ginkgo biloba*

that is widely found in eastern Asia (China, Japan) and has fan-shaped leaves, the other species was *Zelkova serrata*, a tall widely spreading Japanese tree of the elm family. *Ginkgo biloba* and *Zelkova serrata* were selected, because the surface of these leaves is almost flat.

Leaf samples were obtained by cutting small branches from sunlit parts of the canopy using a pruning hook scissors and immediately were sent to the laboratory. The leaves were immediately clipped from the branches and stored in a plastic case containing cold water to maintain its freshness. The leaves were swelled for 1 hr. All measurements of spectral reflectance were completed within 3 hr of picking the leaves. Chlorophyll determination was done immediately by putting the leaf into the organic solvent within 1 hr after measurement of spectral reflectance.

2.2 Measurements of Leaf Spectral Reflectance with Hyperspectral Imager

The measurement of spectral reflectance was carried out in the laboratory darkroom using both the handmade portable hyperspectral imager with AOTF. Also the hyperspectral meter (GER, GER2600) was used to obtain reference spectral data for the imager. This hyperspectral imager consists of three components. The first component is AOTF telescope video adaptor (Brimrose Corporation, TAV-100), which can record incident radiation in a range of 400 – 1000 nm wavelength at user defined wavelength interval. The second component is a supersensitive CCD camera (Photometrics, PXL1400), which has CCD elements of 1320*1027 pixels and 12 bits. The neutral density filter was attached to CCD camera, because of its sensitivity being too high. The third component is the software (IPLab, LPLab PXL), which can control both camera behavior and wavelength range and wavelength resolution. Field of view of this instrument is 10°. Working distance is from 1 m to infinity. In this study, working distance was 2 m vertically from the ground. On the other hand, the GER-2600 records radiation in 650 channels over a range of 333-2500 nm wavelengths. In this study, the spectral reflectance of the leaf was measured between 450 – 1000 nm wavelengths at intervals of 5 nm.

The swelled leaf was put on the black sponge made from ethylene propylene rubber (EP rubber) with a masking tape to reduce noise from the background. Spectral reflectance of EP rubber sponge is very flat with an average of about 2 % in the range of 400 – 1000 nm. In addition, the EP rubber sponge has heat resistance up to 120 °C. Spectral reflectance was calculated using Eq. (1) with the standard white board made from BaSO₄ as the reference. The spectral reflectance image was recalculated as a moving average of 3 wavelengths to reduce noise, as shown in Eq. (2). Besides, after leaf disk was bored to examine relationship between spectral reflectance of leaf disk area and chlorophyll *a* concentration, leaf image was measured again at one single wavelength to determine the bore locations. Geometric correction was done to the calculated spectral reflectance, because the view area of measured images shifts due to AOTF characteristics.

$$RF_i (\%) = \frac{(\text{target}_i - \text{dark current})}{(\text{reference}_i - \text{dark current})} \times 100 \quad (1)$$

where RF_i is reflectance at i nm, reference_i and target_i are the digital value of white board and target at i nm, respectively. Dark current is the initial digital value of CCD elements under a closed shutter of camera.

$$RF_{ra\ i} (\%) = \frac{RF_{i-1} + RF_i + RF_{i+1}}{3} \quad (2)$$

where $RF_{ra\ i}$ is the moving average of RF_i at i nm. Figure 1 shows an example of a hyperspectral image of a leaf (*Ginkgo biloba*).

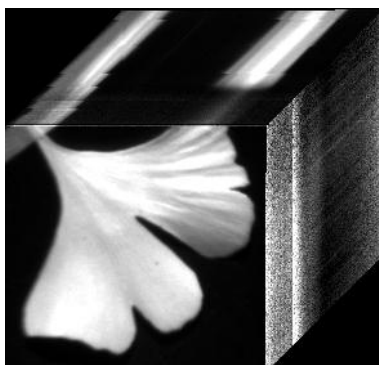


Fig. 1. An example of hyperspectral image of leaves (*Ginkgo biloba*)

2.3 Determination of Chlorophyll *a* Concentration

After the measurement of spectral characteristics of leaf, several leaf disks of 1 cm diameter were precisely bored with a punch. Chlorophyll *a* concentration unit per area could be determined, because the area of leaf disk was a uniform $0.25 \cdot \pi \text{ cm}^2$. The chlorophylls were extracted in 100 % DMF (*N,N'*-dimethylformamide) with a leaf disk. Extractable efficiency of DMF is stronger than that of acetone. The absorption spectrum of the extracted liquid at 663.8 nm and 646.8 nm were measured with a spectrophotometer (HITACHI, U-2010). Chlorophyll *a* concentration ($\mu\text{g/ml}$) was calculated by Eq. (3), (Porra et al., 1989):

$$\text{Chlorophyll } a (\mu\text{g/ml}) = 12.00A^{663.8} - 3.11A^{646.8} \quad (3)$$

where $A^{663.8}$ and $A^{646.8}$ are the absorbance at 663.8 nm and 646.8 nm wavelength, respectively.

2.4 Determination of RWC

The swelled leaf's weight was measured by an electrically scale and the swelled leaf was put on the EP rubber sponge and the total of weight of the swelled leaf and this sponge were measured as initial weight again. Weight and size of the EP rubber sponge was stable under 80°C oven. This sample was put into the drying oven at 80 °C and was removed from the drying oven at several accumulated time intervals. The weight and spectral reflectance of the same sample was measured at 0, 3, 5, 7, 9, 11, 15, 20, 25, 30, 40 min and 24 hr. RWC was calculated by using Eq. (4):

$$\text{RWC}_i (\%) = \frac{\text{weight}_i - \text{weight}_{final}}{\text{weight}_{ini} - \text{weight}_{final}} \times 100 \quad (4)$$

where RWC_i is relative water content at *i* min, weight_{ini} , weight_{final} , weight_i are the total of weight of leaf and sponge at 0min, 24 hr, *i* min, respectively.

3. SPATIAL ESTIMATION OF CHLOROPHYLL *a* CONCENTRATION

3.1 Correlation between Chlorophyll *a* Concentration and Spectral Reflectance

Here, relationship between spectral characteristics of a leaf and chlorophyll *a* concentration was examined with the measured reflectance ((Eq. (2)) and the measured chlorophyll *a* concentration ((Eq. (3)). Reflectance was measured at several points on leaves and chlorophyll *a* concentration was obtained from the sampled leaf disks at the corresponding points where the reflectances were measured. Figure 2 shows an example of a hyperspectral image of a leaf at 780 nm. The spectral reflectances of leaf at the circled area in Fig. 2 are shown in Fig. 3. The deviation of spectral reflectance was quite small in the neighborhood of red edge position than in the other ranges in both red color area and blue color area. The deviation of spectral reflectance at neighborhood of red position for all leaves was the smallest at all wavelengths. Then, the correlation between spectral reflectance and chlorophyll *a* concentration was investigated at the neighborhood of red edge position. Two methods were examined to estimate chlorophyll *a* concentration from spectral reflectance; (1) a correlation between chlorophyll *a* concentration and spectral reflectance at one single wavelength; (2) a correlation between chlorophyll *a* concentration and the first derivative spectral reflectance (RF') at one single wavelength. The first spectral derivative spectral reflectance was calculated by Eq. (5):

$$\text{RF}'_j (\%) = \frac{\text{RF}_{rai+1} - \text{RF}_{rai}}{\lambda_{i+1} - \lambda_i} \quad (5)$$

where λ_i is wavelength, RF'_j is the first derivative spectral reflectance at intermediate wavelength of between λ_{i+1} and λ_i

The correlation between RF_{ra} and chlorophyll *a* concentration is shown in Fig. 4. The correlation coefficient is negatively proportional to the absorption wavelength of chlorophyll *a* ($r=0.69$, at 685nm). However, the correlation coefficient was not too high at all wavelength ranges. The correlation between RF' and chlorophyll *a* concentration was investigated. Fig. 5 shows the correlation between RF' and chlorophyll *a* concentration. The correlation coefficient was too high in the neighborhood of red edge position ($r=0.92$, at 727.5nm), (*Ginkgo biloba*)

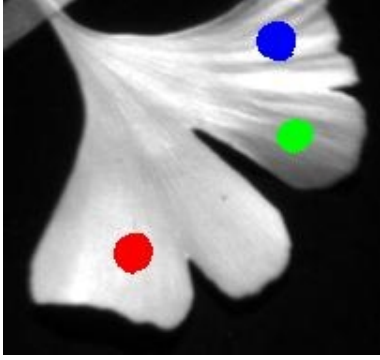


Fig. 2. An example of a hyperspectral image of a leaf at 780 nm. The colored areas show the position where relationship between spectral reflectance and chlorophyll *a* concentration was investigated.
(*Ginkgo biloba*)

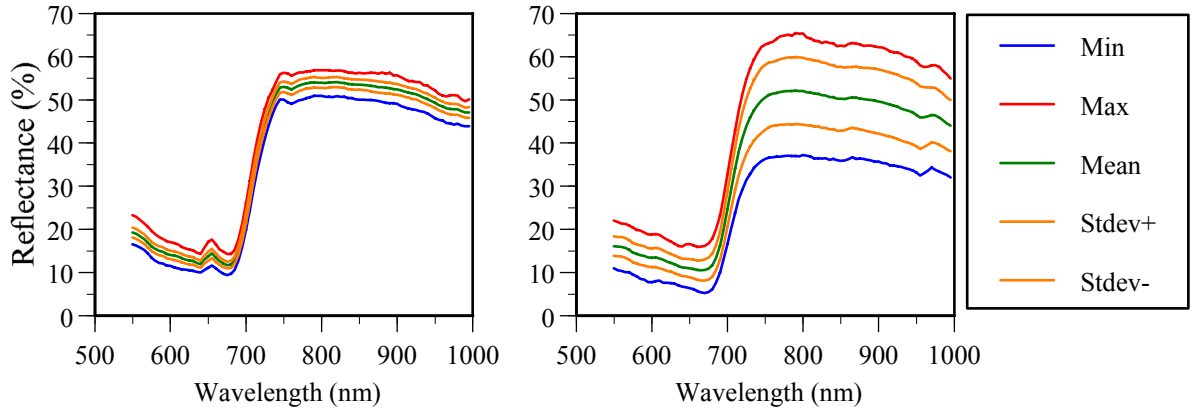


Fig. 3. The spectral reflectance characteristics at red color area (left) and at blue color area (right)

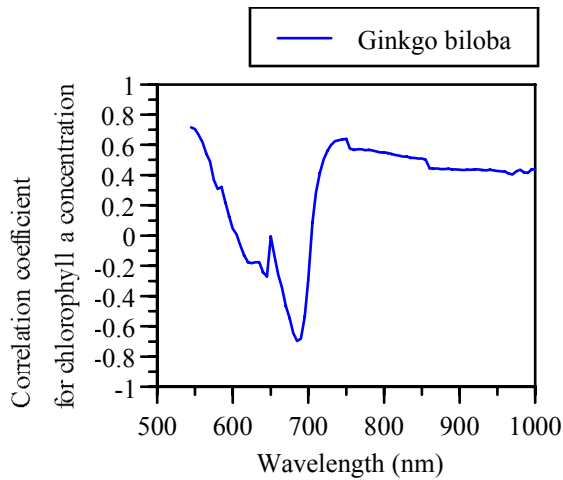


Fig. 4. Correlogram showing the correlation coefficient between RF_{ra} and chlorophyll *a* concentration at each wavelength

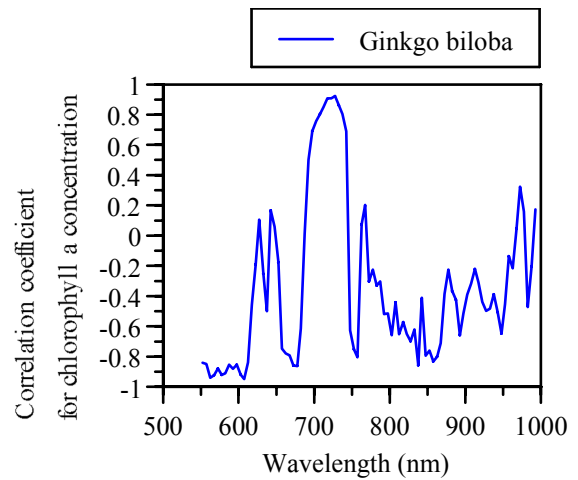


Fig. 5. Correlogram showing the correlation coefficient between RF' and chlorophyll *a* concentration at each wavelength

Chlorophyll *a* concentration of both *Ginkgo biloba* and *Zelkova serrata* were estimated from relationship between chlorophyll *a* concentration and the RF' at the different holes. Each chlorophyll *a* concentration could be estimated by Eq. (6) and Eq. (7):

(1) *Ginkgo biloba*

$$\text{Chlorophyll } a (\mu\text{g} / \text{cm}^2) = 73.28 \times RF'_{727.5} - 1.06 \quad (r^2 = 0.85) \quad (\text{RMS error} = 4.08 \mu\text{g}/\text{cm}^2) \quad (6)$$

(2) *Zelkova serrata*

$$\text{Chlorophyll } a (\mu\text{g} / \text{cm}^2) = 56.63 \times RF'_{732.5} + 8.56 \quad (r^2 = 0.78) \quad (\text{RMS error} = 3.05 \mu\text{g}/\text{cm}^2) \quad (7)$$

where $RF'_{727.5}$ and $RF'_{732.5}$ are the first derivative spectral reflectance at 727.5 nm ,732.5 nm, respectively.

the hyperspectral image including the leaf area was clarified to estimate chlorophyll *a* concentration. Classification of leaf area from image was carried out by the inner product with the standard spectrum of leaf, the EP rubber sponge and the masking tape. Only leaf area was extracted. Fig. 6 and Fig. 7 show the results of the distribution of chlorophyll *a* concentration for *Ginkgo biloba* and *Zelkova serrata*. The results demonstrated that distribution of chlorophyll *a* concentration could be estimated from hyperspectral image. The actual leaf of *Zelkova serrata* was partly dry. In addition, in determination of chlorophyll *a* concentration, the leaf of *Ginkgo biloba* had higher chlorophyll *a* concentration than *Zelkova serrata*. The chlorophyll *a* concentration of the leaf corresponds realistically to the physical structure of it. However, estimation of chlorophyll *a* concentration tended to be underestimated at areas covered by shadow and at surfaces of leaf waving.

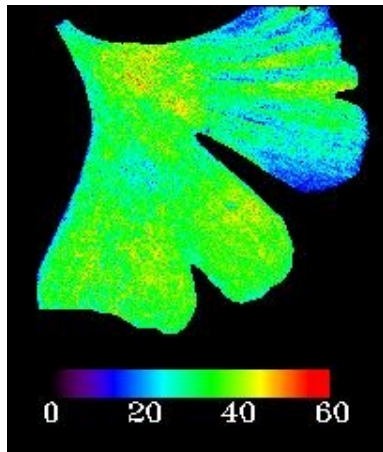


Fig. 6. A distribution of chlorophyll *a* concentration ($\mu\text{g}/\text{cm}^2$) in the leaf of *Ginkgo biloba*

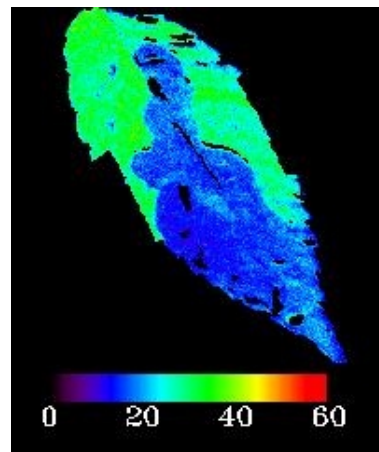


Fig. 7. A distribution of chlorophyll *a* concentration ($\mu\text{g}/\text{cm}^2$) in the leaf of *Zelkova serrata*

3.2 Correlation between RWC and Spectral Reflectance

Each RF_{ra} of *Ginkgo biloba* at accumulated time intervals is shown in Fig. 8. The change of RF_{ra} at a range of 1000 – 2500 nm was bigger than the change of RF_{ra} at a range of 333 – 1000 nm. The RF_{ra} at intermediate infrared domain tended to become higher in proportion to increasing accumulated time. The RF_{ra} of each accumulated intervals at neighborhood of 1500 nm and 1900 nm was obviously affected by water. The correlation between RF_{ra} and RWC was examined for *Ginkgo biloba*, *Zelkova serrata*, respectively (Fig. 9). The correlation coefficient between RWC and RF_{ra} of each of the leaf was too high at over 1400 nm. The feature of correlation coefficient in range of 400 – 1000 nm was different for each of them. Hence, it is difficult to estimate RWC using just the hyperspectral imager only with visible and near infrared spectral range.

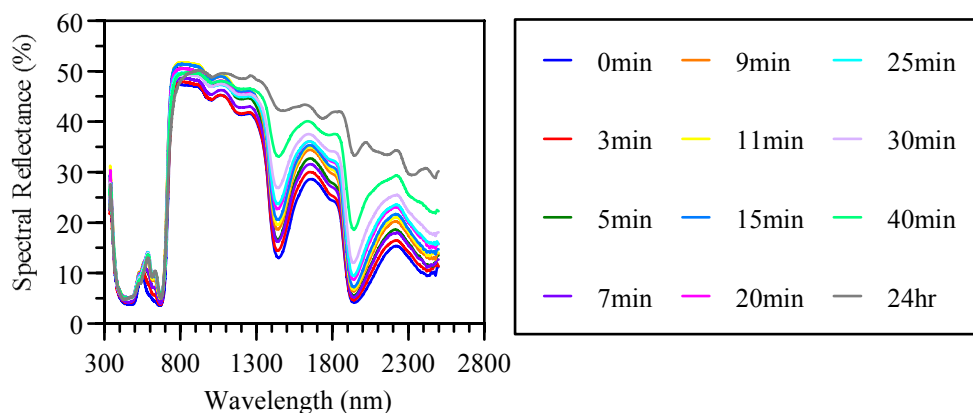


Fig. 8. RF_{ra} of the drying leaf at accumulated time intervals (*Ginkgo biloba*)

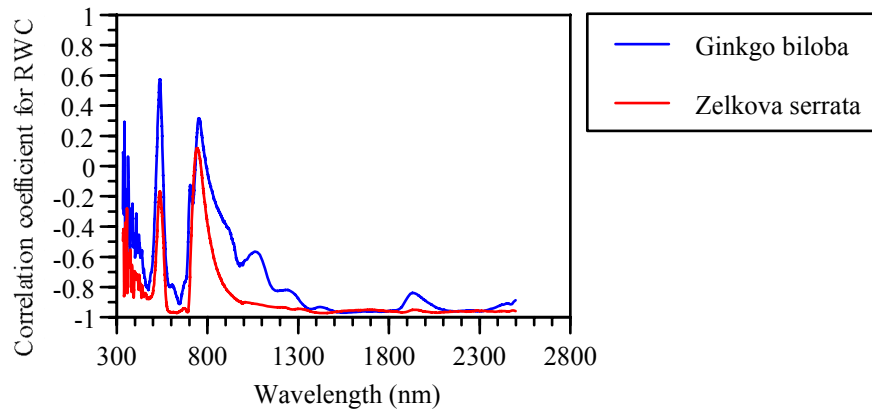


Fig. 9. Correlogram showing the correlation coefficient between RF_{ra} of RWC (*Ginkgo biloba*)

4. CONCLUSIONS

The deviation of spectral reflectance of leaf surface was the smallest at neighborhood of red edge position. The first derivative spectral reflectance at neighborhood of red edge position was a useful to estimate chlorophyll *a* concentration ($\mu\text{g}/\text{cm}^2$). A distribution of chlorophyll *a* concentration of the entire leaf image of both *Ginkgo biloba* and *Zelkova serrata* could be estimated with RMS error of $4.80 \mu\text{g}/\text{cm}^2$, $3.05 \mu\text{g}/\text{cm}^2$, respectively. On the other hand, it was difficult to estimate RWC of leaf from hyperspectral measurement at only visible and near infrared range.

The portable hyperspectral imager is shown to be a useful tool for analyzing hyperspectral images including the effect of shadow, stem and overlap of leaves. In the future, the effect of shadow, stem and overlap of leaves will be examined using the portable hyperspectral imager. In addition, a distribution of nitrogen concentration will also be investigated to estimate photosynthetic activity of the vegetation.

REFERENCES

- Lee F. Johnson, Christine A. Hlacka, and David L. Peterson, 1994. Multivariate Analysis of AVIRIS Data for Canopy Biochemical Estimation along the Oregon Transect. REMOTE SEN. ENVIRON., 47, pp. 216-230.
- Miller, J., Hare, Emery, D. R., and Kerr, C. H. , 1997. Equipment Pool for Field Spectroscopy. Remote Sensing Observations and Interaction, Remote sensing Society, preparing for the 21st In RSS'97, pp. 159-164.
- Paul J. Curran, John A. Kupiec, and Geoffrey M. Smith, 1997. Remote Sensing the Biochemical Composition of a Slash Pine Canopy. IEEE TRANSSACTION ON GEOSCIENCE AND REMOTE SENSING, 35(2),, pp. 415-420.
- R. J. Porra, W. A. Thompson and P. E. Kriedeman, 1989. Determination of Accurate Extinction Coefficients and Simultaneous Equations for Assaying Chlorophylls *a* and *b* extracted with Four Different Solvents: verification of the concentration of chlorophyll standards by atomic absorption spectroscopy. Biochi. mica et Biophysica Acta, 975, pp. 384-394.
- Rosemary A. jago, Mark E. J. Cutler, and Paul J. Curran, 1999. Estimating Canopy Chlorophyll Concentration from Field and Airborne Spectra. REMOTE SEN. ENVIRON., 68(3), pp. 217-224.
- T. Endo, T. Okuda, M. Tamura and Y. Yasuoka, 2000. Estimation of Net Photosynthetic Rate based on In-Situ Hyperspectral Data, SPIE, proceedings of SPIE 4151., pp. 214-221.